FISEVIER

Contents lists available at ScienceDirect

Computational and Theoretical Chemistry

journal homepage: www.elsevier.com/locate/comptc



Diabatic and adiabatic representations: Electronic structure caveats



David R. Yarkony^{a,*}, Changjian Xie^b, Xiaolei Zhu^c, Yuchen Wang^a, Christopher L. Malbon^a, Hua Guo^{b,*}

- ^a Department of Chemistry, Johns Hopkins University, Baltimore, MD 21218, USA
- ^b Department of Chemistry and Chemical Biology, University of New Mexico, Albuquerque, NM 87131, USA
- ^c Department of Chemistry, Stanford University, Stanford, CA 94305, USA

ARTICLE INFO

Keywords: Conical intersections Geometric phase Vector potential Nonadiabatic tunneling Diabatic representations

ABSTRACT

In this Viewpoint issues in the construction and use of adiabatic and diabatic representations in describing spinconserving electronically nonadiabatic processes using the Born-Huang ansatz are reviewed and illustrated. We address issues which limit the accuracy of commonly used approximate equations of motion. The following caveats are discussed. (i) The use of adiabatic states for $N^{state} > 2$ is complicated by the fact that if states (I, J)and (J, K) have conical intersections then the derivative coupling $\mathbf{f}^{(a),I,J}(\mathbf{R})$ may well be double-valued, rendering it inappropriate for nuclear dynamics. (ii) In the nonadiabatic tunneling regime, nuclear motion can be restricted to a single adiabatic potential energy surface on the basis of total energy. However, energetically inaccessible conical intersections make it necessary to take into account the geometric phase and the induced vector potential when formulating the nuclear Schrödinger equation. We review how a diabatization approach which takes explicit account of the derivative couplings can be used to accurately include these factors. (iii) Finally, we review how a commonly used class of two-state diabatizations based on smooth molecular properties can be subject to ruinous singularities inherent in equations defining the diabatization.

In this Viewpoint issues in the construction and use of adiabatic and diabatic representations in describing spin-conserving electronically nonadiabatic processes are reviewed and illustrated. The issues discussed arise mostly, but not exclusively, from the existence of conical intersections (CIs) and the singularities and geometric phase (GP) effects they induce. We begin this Viewpoint with a description of the GP and of the adiabatic state nuclear Schrödinger equations that must be solved to describe nonadiabatic dynamics in the Born-Huang ansatz [1]. In that ansatz, the total wave function is expanded as a sum of products of nuclear and electronic wave functions. The electronic wave functions satisfy an electronic Schrödinger equation. In this approach the picture of molecular evolution on potential energy surfaces (PESs) connected by nonadiabatic events is obtained.

1. The origin of the geometric phase

The adiabatic electronic wave functions satisfy the electronic Schrödinger equation

$$[H^{e}(\mathbf{r}; \mathbf{R}) - E_{J}^{(a)}(\mathbf{R})]\Psi_{J}^{(a)}(\mathbf{r}; \mathbf{R}) = 0$$

$$(1.1)$$

In Eq. (1.1), $\Psi_I^{(a)}(\mathbf{r}; \mathbf{R})$ are taken to be *real-valued*, \mathbf{r} (**R**) denote the

electronic ($3N^{atom}$ nuclear) coordinates and $H^e(\mathbf{r}; \mathbf{R})$ is the electronic Hamiltonian in the non-relativistic Coulomb approximation. Here, the semicolon denotes the fact that the Hamiltonian is parametrically dependent on nuclear coordinates, based on the assumption that electronic motion is significantly faster than nuclear motion [2]. According to the GP theorem [3–5], the real-valued $\Psi_f^{(a)}(\mathbf{r}; \mathbf{R})$ changes sign when transported along a closed loop which contains an odd number of CIs. This double-valued character is anathema and must be removed from the total wave function, $\Psi^{T,n}(\mathbf{r}, \mathbf{R})$, by, for example, a geometry (\mathbf{R}) and state (J) dependent phase factor $e^{iA^{(J)}(\mathbf{R})}$ chosen so that the complex-valued electronic wave function in [] in Eq. (1.2a) below is single-valued as are the nuclear wave functions $\chi_J^{(a),n}(\mathbf{R})$ and hence the total wave function can be written as

$$\Psi^{T,n}(\mathbf{r},\mathbf{R}) = \sum_{J=1}^{N^{state}} \left[\Psi_J^{(a)}(\mathbf{r};\mathbf{R}) e^{iA^{(J)}(\mathbf{R})} \right] \chi_J^{(a),n}(\mathbf{R})$$
(1.2a)

Here, n indexes the nuclear states and we define

$$\widetilde{\Psi}_{J}^{(a)}(\mathbf{r}; \mathbf{R}) = \exp(iA^{(J)}(\mathbf{R}))\Psi_{J}^{(a)}(\mathbf{r}; \mathbf{R})$$
(1.2b)

This GP, $e^{iA^{(J)}(\mathbf{R})}$, is required regardless of the value of N^{state} .

E-mail addresses: yarkony@jhu.edu (D.R. Yarkony), hguo@unm.edu (H. Guo).

^{*} Corresponding authors.

2. The nuclear Schrödinger Equation: Adiabatic state descriptions

The total Hamiltonian can be written as

$$H(\mathbf{r}, \mathbf{R}) = T_N + H^e(\mathbf{r}; \mathbf{R})$$
 (2.1a)

where $\hbar = 1$ throughout and

$$T_N = \sum_{i=1}^{3N^{alom}} \frac{-1}{2M_i} \frac{\partial^2}{\partial R_i^2}$$
 (2.1b)

is the nuclear kinetic energy operator. The form of the working nuclear Schrödinger equation depends on the approximations employed.

2.1. Single adiabatic electronic state approximations

We begin with the single adiabatic state approximation

$$\Psi_K^{T,k}(\mathbf{r}, \mathbf{R}) = \Psi_K^{(a)}(\mathbf{r}; \mathbf{R}) \chi_K^{(a),k}(\mathbf{R})$$
(2.2)

In this approximation, nuclei move on a single adiabatic PES created by the faster moving electrons, $E_{\ell}^{(a)}(\mathbf{R})$, the K^{th} eigenvalue of H^{e} .

In this Born-Oppenheimer approximation (BOA) [2], $\Psi_K^{(a)}(\mathbf{r};\mathbf{R})$ satisfies Eq. (1.1) and $\chi_K^{(a),k}(\mathbf{R})$ satisfies the electronic state dependent nuclear Schrödinger equation

$$[T_N + E_K^{(a)}(\mathbf{R}) - E_K^k] \chi_K^{(a),k}(\mathbf{R}) = 0$$
(2.3)

Eq. (2.3) ignores the **R** dependence of $\Psi_K^{(a)}(\mathbf{r};\mathbf{R})$ when differentiating. When the **R** dependence of $\Psi_K^{(a)}(\mathbf{r};\mathbf{R})$ is included, we have the adiabatic state approximation

$$[T_N + E_K^{(a)}(\mathbf{R}) + \sum_{i=1}^{3N^{alom}} \frac{G_{i,i}^{(a),K,K}(\mathbf{R})}{2M_i} - E_K^k] \chi_K^{(a),k}(\mathbf{R}) = 0$$
(2.4a)

where

$$G_{i,i}^{(a),K,K}(\mathbf{R}) = -\left\langle \Psi_K^{(a)}(\mathbf{r}; \mathbf{R}) | \frac{\partial^2}{\partial R_i^2} \Psi_K^{(a)}(\mathbf{r}; \mathbf{R}) \right\rangle_{\mathbf{r}} = k_{i,i}^{(a),K,K}(\mathbf{R})$$
(2.4b)

$$\left\langle \Psi_{J}^{(a)}(\mathbf{r}; \mathbf{R}) | \frac{\partial^{2}}{\partial R_{i}^{2}} \Psi_{K}^{(a)}(\mathbf{r}; \mathbf{R}) \right\rangle_{\mathbf{r}} + k_{i,i}^{(a)J,K} = \frac{\partial}{\partial R_{i}} f_{i}^{(a)J,K}$$
(2.5a)

the derivative coupling is defined as

$$f_{i}^{(a)J,K} = \left\langle \Psi_{J}^{(a)}(\mathbf{r}; \mathbf{R}) | \frac{\partial}{\partial R_{i}} \Psi_{K}^{(a)}(\mathbf{r}; \mathbf{R}) \right\rangle_{\mathbf{r}}$$
(2.5b)

and

$$k_{i,i}^{(a),J,K} = \left\langle \frac{\partial}{\partial R_i} \Psi_J^{(a)}(\mathbf{r}; \mathbf{R}) | \frac{\partial}{\partial R_i} \Psi_K^{(a)}(\mathbf{r}; \mathbf{R}) \right\rangle_{\mathbf{r}}$$
(2.5c)

For J=K, $\sum_{i=1}^{3N^{alom}} \frac{1}{2M_i} k_{i,i}^{(a),K,K}$ is the Diagonal Born-Oppenheimer Correction (DBOC) [6] and is singular at a CI.

2.2. Coupled adiabatic electronic states

2.2.1. Conical intersections absent

When $N^{state}>1$ and no CIs are present so the GP need not be considered, the total wave function has the form

$$\Psi^{T,k}(\mathbf{r},\mathbf{R}) = \sum_{K=1}^{N^{state}} \Psi_K^{(a)}(\mathbf{r};\mathbf{R}) \chi_K^{(a),k}(\mathbf{R})$$
(2.6)

Projecting the total Schrödinger equation $H\Psi^{T,k} = \Psi^{T,k}E^k$ onto $\Psi^{(a)}_J$ for all J gives the system of N^{state} coupled equations:

$$\sum_{K=1}^{N^{state}} \left[\sum_{i=1}^{3N^{atom}} \frac{-1}{2M_{i}} \left(\delta_{J,K} \frac{\partial^{2}}{\partial R_{i}^{2}} + 2f_{i}^{(a),J,K} \frac{\partial}{\partial R_{i}} + G_{i,i}^{(a),J,K} \right) + E_{J,K}^{(a)}(\mathbf{R}) \right] \chi_{K}^{(a),k}$$

$$= \chi_{J}^{(a),k} E^{k}$$
(2.7a)

Here

$$E_{K,L}^{(a)}(\mathbf{R}) = \delta_{K,L} E_K^{(a)}(\mathbf{R}) \tag{2.7b}$$

and $\mathbf{f}^{(a)}$ is a matrix in the state indices (J, K) and a vector in the coordinate indices (i) $[f_i^{(a),J,K}]$. This form of the nuclear Schrödinger equation, often without the DBOC term [7] is frequently used in surface hopping [8] treatments of nuclear dynamics.

2.2.2. Conical intersections present

When CIs exist, the GP must be included, at least formally. Including the GP in the wave function leads to a nuclear Schrödinger equation of the form [9,10] [\forall I]

$$\begin{cases}
\sum_{i=1}^{3N^{allom}} \frac{1}{2M_{i}} [(p_{i} + A_{i}^{(I)})^{2} + k_{i,i}^{(a),I,I}] + E_{i}^{(a)} - E^{k} \\
\sum_{I}^{N^{state}} e^{iA^{(I,I)}} \sum_{i=1}^{3N^{allom}} \frac{1}{2M_{i}} [f_{i}^{(a),I,J} i(p_{i} + A_{i}^{(J)}) + i(p_{i} + A_{i}^{(J)}) f_{i}^{(a),I,J} \\
+ k_{i,i}^{(a),I,J}]\chi_{J}^{(a),k},
\end{cases} (2.8)$$

where in Eq. (2.8)

$$A_{j}^{(I)}(\mathbf{R}) \equiv \frac{\partial}{\partial R_{j}} A^{(I)}(\mathbf{R}); \quad A^{(I,I)} = A^{(I)} - A^{(I)}; \quad p_{j} = -i \frac{\partial}{\partial R_{j}}$$

$$(2.9)$$

and $A_i^{(K)}$ is the vector potential (VP) [4]. The nuclear Schrödinger equation in Eqs. (2.8) and (2.9) can be used to determine how the GP impacts nuclear motion in the adiabatic representation [7,9,11–13]. Indeed, recent studies of the GP effects [10,14–23] in reactive systems treat it using variants of this VP approach which was originally introduced by Mead and Truhlar [4].

2.2.3. $N^{state} = 1$. The molecular Aharonov-Bohm effect limit

Of particular recent interest is the perhaps incongruous limit of Eq. (2.8) when $N^{state}=1$. This limit is valid as long as the state in question is well separated from the remainder of the Hilbert space. Current interest centers around the situation where the CI seam is energetically inaccessible. The appellation Molecular Aharonov-Bohm (MAB) effect limit was introduced by Mead and Truhlar [4,24] based on the conceptual similarities between the AB effect, which describes the phase an electron acquires in a vanishing magnetic field [25], and the GP induced by a CI in the single adiabatic state representation. In this case the nuclear Schrödinger equation becomes

$$\begin{cases} \sum_{i=1}^{3N^{atom}} \frac{1}{2M_i} \left[\left(-i \frac{\partial}{\partial R_i} + A_i^{(I)} \right)^2 + k_{i,i}^{(a),I,I} \right] + E_I^{(a)}(\mathbf{R}) - E_I^k \end{cases} \chi_I^{(a),k} = 0 \tag{2.10}$$

Eq. (2.10) differs from the single adiabatic state nuclear Schrödinger Eq. (2.4) by the VP $A_i^{(I)}$. This limit includes the "indirect effects" of the CI, that is the effects required by single valuedness.

In Section 4, we explain how $A_i^{(I)}$ required for this limit can be deduced from the derivative coupling with $N^{state} = 2$.

2.3. User's guide to the adiabatic state nuclear Schrödinger equation

In the previous Sections, four distinct nuclear Schrödinger equations have been introduced. Eq. (2.3) which has a simple form of the kinetic energy and Eq. (2.4) which includes the DBOC, have $N^{state} = 1$. Eq. (2.7) is diagonal in the electronic energy and couples N^{state} electronic states through the derivative coupling and to a much smaller extent the second derivative coupling. Since $\Psi_J^{(a)}$ are real-valued, it assumes no CIs are present, as is the case in diatomic molecules. Eq. (2.8) is the most general adiabatic state nuclear Schrödinger equation including the

effects of CIs and the induced GP. It however has significant technical issues with both its formulation and solution. See below and Section 5.3. Eq. (2.10), originally introduced by Mead and Truhlar in the context of the MAB effect [4,24] is the $N^{state} = 1$ form of Eq. (2.8). Recently it has been found most useful in describing the effects of energetically inaccessible CIs [10].

The VP in Eq. (2.9) is required regardless of whether or not the CI seam giving rise to it is energetically accessible. The DBOC and VP are both singular at the CI and the single electronic state nuclear Schrödinger equation, Eq. (2.10), will have an extended node leading to the CI [9,10,26]. This should be contrasted with the solution to Eq. (2.3) usually used to describe standard single state dynamics which has no such node [10]. Although this change in the nodal structure of the nuclear wave function is dramatic, the DBOC and VP are infrequently included in single state dynamics since their need is difficult to anticipate and the VP is difficult to construct in the general case. In Section 4, a method of constructing the VP based on *ab initio* wave functions is reviewed [27].

3. Diabatic electronic states

This section introduces the diabatic representation of the electronic states. A disadvantage of the diabatic representation is that it requires at least two states even for a situation in which the single adiabatic state approximation is expected to hold. More significant is the fact that it cannot, except in a limited set of cases, be uniquely defined, with no guarantee that distinct representations will yield the same nuclear dynamics.

3.1. Diabatic representations

The diabatic representation is a unitary transformation of the adiabatic electronic states

$$\Psi_{\alpha}^{(d)}(\mathbf{r};\mathbf{R}) = \sum_{K=1}^{N^{\text{state}}} \mathbf{U}(\mathbf{R})_{K,\alpha} \Psi_{K}^{(a)}(\mathbf{r};\mathbf{R})$$
(3.1a)

where to preserve the form of wave function in Eq. (2.6) we require

$$\chi_{\alpha}^{(d)}(\mathbf{R}) = \sum_{K=1}^{N^{\text{state}}} \mathbf{U}(\mathbf{R})_{\alpha,K}^{\dagger} \chi_{K}^{(a)}(\mathbf{R})$$
(3.1b)

If **U** is chosen such that

$$\left\langle \Psi_{I}^{(d)}(\mathbf{r}; \mathbf{R}) | \frac{\partial}{\partial R_{k}} \Psi_{J}^{(d)}(\mathbf{r}; \mathbf{R}) \right\rangle_{\mathbf{r}} = 0 \text{ for all } (I < J) \text{ and } R_{k},$$
(3.2)

then U satisfies the system of partial differential equations in the coordinates (see Appendix A, Eq. (A.6))

$$\nabla_{\mathbf{R}}\mathbf{U}(\mathbf{R}) + \mathbf{f}(\mathbf{R})\mathbf{U}(\mathbf{R}) = \mathbf{0} \tag{3.3}$$

where $\nabla_{\mathbf{R}} \equiv \frac{\partial}{\partial R_1}, \frac{\partial}{\partial R_2}, ..., \frac{\partial}{\partial R_{3N} atom}$ and the nuclear Schrödinger in the diabatic basis is

$$\left[-\sum_{i=1}^{3N^{atom}} \frac{1}{2M_i} \frac{\partial^2}{\partial R_i^2} \mathbf{I} + \mathbf{U}^{-1} \mathbf{E}^{(a)} \mathbf{U} - E \mathbf{I}\right] \chi^{(d)} = 0$$
(3.4)

It is useful to recall the connections between Eqs. (3.2), (3.3), and (3.4) and the adiabatic nuclear Schrödinger equations. These equations are tied together by the curl condition which describes (see Appendix B) when Eq. (3.3) has a solution in which case the kinetic energy is diagonal (Eq. (3.4)). The curl condition has been carefully studied [28–30]. Eq. (3.3) only has a solution in general when there is one internal coordinate, that is for diatomic molecules, or when the dimension of the electronic Hilbert space, N^{es} , is N^{state} . Since in this case Eq. (3.3) holds, we say f is removable, since there is no derivative coupling in the diabatic representation.

We have the following conundrum concerning the use of the Born-Huang expansion to represent a nonadiabatic wave function based on accurate ab initio solutions to Eq. (1.1). On the one hand, the DBOC singularity at the CI requires the wave function to die off rapidly in the vicinity of the CI for its matrix elements to be integrable [31,32]. Depending on the energy of the CI the matrix elements of the DBOC may be infinite, precluding the determination of most or all of the eigenstates in the adiabatic representation. On the other hand, the eigenstates of Eq. (3.4) are comparatively easy to determine [33]. However, in this case the adiabatic to diabatic states (AtD) transformation cannot be done exactly owing to the failure of curl condition for ab initio wave functions. Thus, solutions to Eq. (3.4) are an exact solution to an approximate problem owing to the absence of exact solutions to Eq. (3.3). Solutions to Eq. (2.8) provide for approximate solutions to an "exact" problem, since the DBOC singularities cannot be treated at total energies that are too high. Adiabatic state data result in an additional issue for $N^{state} > 2$, double-valued derivative couplings (see Section 5.3) [34]. However, in favorable circumstances (for $N^{state} = 2$), it is possible to construct descriptions which approximate ab initio adiabatic state data and for which the AtD transformation is exact. This issue is discussed in Section 4, using a diabatization scheme discussed below.

3.2. Catalog of methods

The AtD transformation U is an essential tool in nonadiabatic dynamics. U is an $N^{state} \times N^{state}$ orthogonal (almost everywhere) transformation, mapping the well-defined adiabatic states, solutions to Eq. (1.1), into single-valued diabatic states, states for which the residual derivative coupling, the derivative coupling in the diabatic representation, vanishes everywhere. If N^{es} , the dimension of the entire electronic space, is equal to N^{state} , this requirement is achievable [35]. However, for $N^{es} > N^{state}$ the residual derivative couplings cannot be made to vanish exactly (i.e., the derivative couplings are non-removable) [29,36]. It is this inability to eliminate the residual coupling, that has led to the plethora of methods for determining quasi-diabatic states, that is, states for which the residual couplings are small, but do not vanish globally. Such methods include diabatizations based on configuration uniformity [37-41], molecular properties [42,43], localized charges [44,45], least squares minimization of the residual couplings [46,47], block diagonalization [48,49], the regularized diabatic representation [50], global diabatization angle [51], and ansatz [52,53].

The work reviewed here explicitly considers two kinds of diabatization, the simultaneous diabatization-and-fit approach of Zhu and Yarkony (ZY) [54] and the charge localization method known as Boys Localization (BL) as described by Subotnik, Ratner, and their coworkers [44,45]. The analysis of the BL method is generally applicable to smooth molecular properties (Hermitian operator) based diabatizations which include the D-Q and D-Q- Φ methods of Truhlar and coworkers [55,56], and the diabatizations of Mulliken-Hush [43] and of Werner and Meyer [42].

For the commonly encountered situation of 2 states, Θ , the rotation angle, (see Section 3.4) has the property that the defining equations for Θ exhibit singularities in a space of dimension N^{int} -2, (where N^{int} is the number of internal coordinates), that is a space of the same dimension as the seam of CIs, but distinct in form. In Section 5.1, we consider this singular situation numerically.

3.3. A Derivative coupling based diabatization

The diabatization method of Zhu and Yarkony (ZY) [57,58] uses energies, energy gradients, and energy difference scaled derivative couplings to construct an $N^{state} \times N^{state}$ quasi-diabatic model Hamiltonian, \mathbf{H}^d representing N^{state} coupled adiabatic electronic states. Here, the attribute *quasi* denotes the fact that the *ab initio* derivative coupling being fit has a non-removable part. The \mathbf{H}^d itself has no non-removable

part and is in fact strictly diabatic as will be explained in Section 4. \mathbf{H}^d thus represents a removable approximation to the *ab initio* data. The fact that the derivative coupling is explicitly included in the fit lends credibility to its use in constructing the GP/VP, which is discussed in Section 4.

3.3.1. Formulation

For N^{state} adiabatic states each matrix element of the approximating $N^{state} \times N^{state}$ diabatic Hamiltonian, \mathbf{H}^d is expanded as a linear combination of symmetry adapted products of monomials with coefficients of combination V_I so that is \mathbf{H}^d has the form

$$\mathbf{H}^{d}(\mathbf{q}) = \sum_{l=1}^{N^{ef}} V_{l} [\bar{P}^{\kappa[u(l),v(l)]} g^{(l)}(\mathbf{q})] \mathbf{B}^{u(l),v(l)}$$
(3.5)

where **q** denote the $3N^{atom}$ -6 internal coordinates, $\mathbf{B}^{u,v}$ is an $N^{state} \times N^{state}$ symmetric matrix with a 1 in the (u,v) and (v,u) elements and the remaining elements 0; \bar{P}^{x} is a standard group theoretical projection operator for the complete nuclear permutation inversion (CNPI) group; and $g^{(l)}(\mathbf{q})$, $1 \le l \le N^{cf}$, are the monomial basis functions of nuclear coordinates, products of single coordinate functions, described below with N^{cf} the total number of monomials. The constants V_l are determined by the fitting procedure. Accompanying \mathbf{H}^d is an electronic Schrödinger equation

$$\left[\mathbf{H}^{d}(\mathbf{q}) - \mathbf{I}E_{J}^{(a),(m)}(\mathbf{q})\right]\mathbf{d}^{J}(\mathbf{q}) = \mathbf{0}$$
(3.6)

which determines the adiabatic energies $E_J^{(a),(m)}(\mathbf{q})$, energy gradients $E_{J,k}^{(a),(m)}(\mathbf{q}) \equiv \nabla_{R_k} E_J^{(a),(m)}(\mathbf{q})$, and derivative couplings $\mathbf{f}^{(a),J,K,(m)}(\mathbf{q}) = \mathbf{d}^J(\mathbf{q})^\dagger \nabla_q \mathbf{d}^K(\mathbf{q})$. The AtD transformation is given by $\mathbf{d}^{(d)\dagger}$, where $d_{u,l}^{(d)} = d_u^I$ [57,58], that is

$$\Psi_{u}^{d}(\mathbf{r}, \mathbf{q}) = \sum_{J=1}^{N^{state}} \Psi_{J}^{a,(ab)}(\mathbf{r}; \mathbf{q})(\mathbf{d}^{(d)})_{J,u}^{\dagger}(\mathbf{q}) = \sum_{J=1}^{N^{state}} \Psi_{J}^{a,(ab)}(\mathbf{r}; \mathbf{q})\mathbf{d}_{u}^{J}(\mathbf{q})$$
(3.7)

Here, the superscripts a, d, m and ab stand for adiabatic, diabatic, model, and ab initio, respectively. For ease of reference, we define for $1 \le j \le N^{int} = 3N^{atom} - 6$, $1 \le n \le N^{point}$, and (x) = (ab) or (m)

$$L_0^{J,J,(x)}(\mathbf{q}^n) = E_I^{(a),(x)}(\mathbf{q}^n), \tag{3.8a}$$

$$L_j^{J,J,(x)}(\mathbf{q}^n) = \nabla_j E_J^{(a),(x)}(\mathbf{q}^n),$$
 (3.8b)

$$L_j^{J,K,(m)}(\mathbf{q}^n) = \mathbf{d}^J(\mathbf{q}^n)^{\dagger} \nabla_j \mathbf{H}^d \mathbf{d}^K(\mathbf{q}^n), \tag{3.8c}$$

$$L_j^{J,K,(ab)}(\mathbf{q}^n) = (E_K^{(a),(ab)}(\mathbf{q}^n) - E_J^{(a),(ab)}(\mathbf{q}^n))f_j^{(a),J,K,(ab)}(\mathbf{q}^n),$$
(3.8d)

where $\mathbf{f}^{(a),J,K,(ab)}$ is the *ab initio* determined adiabatic derivative coupling.

3.3.2. Defining equations

With the residuals of the energies, energy gradients, and energy difference scaled derivative couplings given respectively by

$$P_0^{J,J}(\mathbf{q}^n) = L_0^{J,J,(ab)}(\mathbf{q}^n) - L_0^{J,J,(m)}(\mathbf{q}^n), \tag{3.9a}$$

$$P_{j}^{J,J}(\mathbf{q}^{n}) = L_{j}^{J,J,(ab)}(\mathbf{q}^{n}) - L_{j}^{J,J,(m)}(\mathbf{q}^{n}), \tag{3.9b}$$

$$P_{j}^{J,K}(\mathbf{R}^{n}) = L_{j}^{J,K,(ab)}(\mathbf{q}^{n}) - L_{j}^{J,K,(m)}(\mathbf{q}^{n}),$$
 (3.9c)

the V_n are chosen to minimize

$$L = \sum_{\substack{k=0,N^{int}\\n=1,Npoint\\1\leqslant l\leqslant N^{State}}} P_k^{J,K}(\mathbf{q}^n)^2$$

$$1\leqslant l\leqslant J\leqslant N^{State}$$
(3.10)

The details of the generation of the fit points \mathbf{q}^n $1 \le n \le N^{point}$ and the solution of the least squares equations is discussed in Refs. [57,58].

3.4. Diabolical singular points

For two-state diabatizations using the BL or properties (Hermitian operator) based diabatizations, care must be exercised to avoid diabolical singular points (DSPs). As we discuss below, DSPs arise from singularities in the equations defining the AtD transformation. At these points the derivative coupling is infinite although the adiabatic states are well separated. DSPs have been analyzed in two recent publications by Zhu and Yarkony [59,60]. There, it is pointed out that many of the commonly used diabatization procedures suffer from ruinous singularities inherent in the equations defining the procedures. A more recent work [61] reports a procedure for locating DSPs and is summarized here.

For two states, the AtD transformation is given by

$$\begin{pmatrix} \Psi_{\alpha}^{(d)}(\mathbf{r}; \mathbf{q}) \\ \Psi_{\beta}^{(d)}(\mathbf{r}; \mathbf{q}) \end{pmatrix} = \begin{pmatrix} \cos\Theta(\mathbf{q}) & -\sin\Theta(\mathbf{q}) \\ \sin\Theta(\mathbf{q}) & \cos\Theta(\mathbf{q}) \end{pmatrix} \begin{pmatrix} \Psi_{I}^{(a)}(\mathbf{r}; \mathbf{q}) \\ \Psi_{J}^{(a)}(\mathbf{r}; \mathbf{q}) \end{pmatrix}$$
(3.11a)

The rotation angle Θ is obtained from

$$\tan m\Theta(\mathbf{q}) = \frac{n(\mathbf{q})}{d(\mathbf{q})}$$
 for $m = 2$ or 4. (3.11b)

where $n(\mathbf{q})$ and $d(\mathbf{q})$ are the numerator and denominator respectively used to define $\tan m\Theta(\mathbf{q})$ and depend on the method of diabatization. Section 5 provides an example. From Eq. (3.11b), $\mathbf{U}(\Theta(\mathbf{q}))$ has the property that the defining equation for Θ exhibits singularities at the \mathbf{q} for which

$$n(\mathbf{q}) = d(\mathbf{q}) = 0, (3.12)$$

in a space of dimension N^{int} -2. The key point here is that this diabolical singularity, is not associated with a near degeneracy of the electronic states and therefore its existence and effects, fallacious large derivative couplings in the adiabatic representation [60] and discontinuities in the diabatic representation [59], may be difficult to anticipate and remove or move to a dynamically irrelevant region.

Since Eq. (3.12) defines a space of dimension N^{int} -2, we introduce auxiliary conditions to define a unique solution in the space of internal coordinates. In particular, we define M^c geometric conditions $K_i(\mathbf{q}) = 0$ $1 \le i \le M^c$ and require that $E_I^{(a)}(\mathbf{q})$ be an extremum. This constrained optimization is solved using the following, Lagrangian,

$$L_{P}(\mathbf{q}, \lambda_{1}, \lambda_{2}, \kappa_{1}, ... \kappa_{M^{c}}) = E_{P}^{(a)}(\mathbf{q}) + \lambda_{1} n(\mathbf{q}) + \lambda_{2} d(\mathbf{q}) + \sum_{i=1}^{M^{c}} \kappa_{i} K_{i}(\mathbf{q})$$
(3.13)

where P = I or J. Optimizing L_P with respect to \mathbf{q} , λ_1 , λ_2 and κ_i ($1 \le i \le M^c$) gives the following system of equations at second order:

$$\begin{pmatrix}
\nabla \nabla L_{p} & (\nabla n, \nabla d) & (\nabla \mathbf{K}) \\
(\nabla n)^{\dagger} & 0 & 0 \\
(\nabla d)^{\dagger} & 0 & 0 \\
(\nabla \mathbf{K})^{\dagger} & 0 & 0
\end{pmatrix}
\begin{pmatrix}
\delta \mathbf{q} \\
\delta \lambda_{1} \\
\delta \lambda_{2} \\
\delta \kappa
\end{pmatrix} = -\begin{pmatrix}
\nabla L_{p} \\
n \\
d \\
\mathbf{K}
\end{pmatrix}$$
(3.14)

where $\nabla^\dagger=(rac{\partial}{\partial q_1},...,rac{\partial}{\partial q_N^{int}}).$ Note the final three equations in Eq. (3.14) are

$$\nabla n(\mathbf{q}) \cdot \delta \mathbf{q} = -n(\mathbf{q}) \qquad n(\mathbf{q}) + \nabla n(\mathbf{q}) \cdot \delta \mathbf{q} = 0$$
 (3.15a)

$$d(\mathbf{q}) + \nabla d(\mathbf{q}) \cdot \delta \mathbf{q} = 0 \tag{3.15b}$$

$$K_i(\mathbf{q}) + \nabla K_i(\mathbf{q}) \cdot \delta \mathbf{q} = 0 \tag{3.15c}$$

which serve to locate a DSP and satisfy the geometric constraints and thus are essential.

 ∇n and ∇d are evaluated using divided difference differentiation based on centered differences as are the first derivatives ∇L_P and second derivatives of the Lagrangian

$$\nabla_i \nabla_j L_P \approx \delta_{i,j} \nabla_i^2 L_P \ 1 \leqslant i, j \leqslant N^{int}$$
(3.16)

Both the first and diagonal second derivatives are accurate to order $O(\delta q_i)^2$ using N^{int} centered differences around each q_i . While the gradients ∇L_P are required for the solution of Eq. (3.14), approximating the matrix $\nabla_i \nabla_j L_P$, by its diagonal elements, second derivatives with respect to q_i , is optional but was found to greatly facilitate optimization of E_P .

4. Single-valued adiabatic representations based on accurate ab initio data

In this section, we use a removable approximation to *ab initio* determined derivative couplings to determine the geometry dependent phase $[\exp(iA^{(K)}(\mathbf{R}))]$ introduced in Section 1 to make the total wave function in the adiabatic representation single-valued [27]. This geometry dependent phase, GP, also known as Berry's phase [5], gives rise to the VP, introduced in Section 2.2, Eq. (2.9). The GP is the sign change incurred by a real-valued adiabatic electronic wave function transported continuously along a closed loop containing a CI. Determining a coordinate system with which to define the loop and corresponding adiabatic potentials is a key issue in treating this effect. Specialized coordinate systems exist for X_3 reactive systems [4,21,24,62-64] owing to their high symmetry. For systems that lack symmetry accurate representations are more challenging. Here we review a recently introduced approach [27] which can treat the general $N^{state} = 2$ case of Eq. (2.8) and its $N^{state} = 1$ limit, Eq. (2.10).

This approach has allowed us to treat the insidious case (recently reviewed [65]) referred to as nonadiabatic tunneling [10,66,67], an example of the MAB effect. Nonadiabatic tunneling is a quantum effect arising from interference among "trajectories" following the different paths around an energetically inaccessible CI in route to dissociation. The tunneling nuclear motion is restricted to a single Born-Oppenheimer PES, but, as it dissociates it can tunnel under either of two equivalent saddle points, which flank the CI. The usual treatment based on Born-Oppenheimer dynamics using Eq. (2.3), is flawed since it does not account for the GP induced by the energetically inaccessible points of CI.

The determination of $A^{(K)}(\mathbf{R})$, for use in Eqs. (2.8) or (2.10) follows from the fact that the line integral of the derivative coupling along an infinitesimal loop equals π when the loop contains a CI and the wave function changes sign after traversing that loop. The line integral is 0 when the loop does not contain a CI. Since $e^{i\pi}=-1$ and $e^{i0}=1$ the infinitesimal circulation (line integral along an infinitesimal closed loop $\oint \mathbf{f}^{(a),I,J,(w)}(\mathbf{R}')\cdot d\mathbf{R}'$) constitutes the geometry dependent phase needed to make the electronic wave function singled-valued. Thus defining,

$$A^{(K)}(\mathbf{R}) = \int_{\mathbf{R}^0}^{\mathbf{R}} \mathbf{f}^{(a),I,J,(w),(\mathbf{R}')} \cdot d\mathbf{R}'$$
(4.1)

where for K=I or J and w=ab for ab initio or m for model, $\Psi_K^{(a),(w)}({\bf r};{\bf R})\exp\left[iA^{(K)}({\bf R})\right]$ is single-valued provided the path remains infinitesimally close to the CI. It is necessary to extend this result to arbitrary paths. The result comes from an unexpected source, the AtD transformation. For $N^{state}=2$ using Eq. (3.11a), Eq. (4.2) becomes

$$\nabla\Theta(\mathbf{R}) = -\mathbf{f}^{(a),I,J,(w)}(\mathbf{R}) \tag{4.2}$$

where for w=m or ab and Θ is defined in Eq. (3.11a). Eq. (4.2) can be used in two ways. With w=ab, the ab initio derivative couple defines $\nabla\Theta$. Since the ab initio derivative coupling is not curl free, see Appendix B, Eq. (4.2) has no solution. However, if $\nabla\Theta$ is taken from the model Hamiltonian \mathbf{H}^d the derivative coupling $\mathbf{f}^{(a),I,J,(m)}(\mathbf{R})$ defined in this way is conservative also termed removable [29], since the AtD transformation eliminates (removes) it. Thus, the derivative coupling is removable provided Θ defines \mathbf{f} . From an alternative perspective, $\mathbf{f}^{(a),I,J,(m)}(\mathbf{R})$ is a removable approximation to the non-removable $\mathbf{f}^{(a),I,J,(ab)}(\mathbf{R})$.

Using Eq. (4.2) and a standard result for line integrals from vector calculus, we demonstrate the path independence of the line integral in Eq. (4.2), for paths that remain in the simply connected domain that excludes the CIs. Multiplying both sides of Eq. (4.2) by $d\mathbf{R}'_i$, summing on i, and integrating from \mathbf{R}^0 to \mathbf{R} gives

$$\int_{\mathbf{R}^{0}}^{\mathbf{R}} \left[\sum_{i=1}^{3N^{alom}} \mathbf{f}_{i}^{(a),I,J,(w)}(\mathbf{R}'_{i}) \cdot \mathbf{d}\mathbf{R}'_{i} \right] = \int_{\mathbf{R}^{0}}^{\mathbf{R}} \left[\sum_{i=1}^{3N^{alom}} \nabla_{i} \Theta(\mathbf{R}'_{i}) \cdot \mathbf{d}\mathbf{R}'_{i} \right]$$
(4.3a)

Using t to parametrize the path, and recognizing that the right-hand side is an exact differential gives

$$= \int_{\mathbf{R}^{0}}^{\mathbf{R}} \left[\sum_{i=1}^{3N^{alom}} \nabla_{i} \Theta(\mathbf{R}') \cdot \frac{\partial \mathbf{R}'_{i}}{\partial t} \right] dt = \int_{0}^{t} \frac{d}{dt} \Theta(\mathbf{R}(t)) dt = \Theta(\mathbf{R}(t)) - \Theta(\mathbf{R}(0))$$
(4.3)

Thus, if Θ satisfies Eq. (4.2), then the line integral of the derivative coupling, the left-hand side of Eq. (4.3a) depends only on its end points, not its path. The converse is also true. Thus $\exp\left(i\int\limits_{R}^{R}\mathbf{f}^{(a),I,J,(w)}(\mathbf{R}')\cdot d\mathbf{R}'\right)$, Eq. (4.1), is path independent if and only if $\mathbf{f}^{(a),I,J,(m)}^{R^0}$ is defined by an Eq. (4.2). Here the singularities have been removed. The contributions from the singularities (CIs) are -1 if the infinitesimal loop contains a CI and 1 otherwise. These observations are demonstrated numerically in Section 5.

5. Constructing the nuclear Schrödinger equation: Caveats

5.1. Diabolical singular points: Properties and loci

The existence of DSPs can invalidate a specific diabatization. Thus, it is essential to be able determine the loci of DSPs before using that diabatization. Here we review the determination of the location and the properties of DSPs using data for 1,2¹A states of NH₃ [60] and its methyl substituted analogue methylamine CH₃NH₂ [61] each reported previously. The diabatization used is the BL approach [44]. This diabatization introduced by Subotnik, Ratner, and coworkers is defined in terms of matrix elements of the three components of the dipole operator $\overrightarrow{\mu} = (\mu_v, \mu_v, \mu_z)$ as follows

$$\mathbf{O}_{I,J}(\mathbf{q}) = \langle \Psi_I^{(a)}(\mathbf{r}; \mathbf{q}) | \overrightarrow{\mu} | \Psi_I^{(a)}(\mathbf{r}; \mathbf{q}) \rangle_{\mathbf{r}}$$
 (5.1a)

$$\bar{\mathbf{G}}_{I,J}(\mathbf{q}) = \mathbf{O}_{I,I}(\mathbf{q}) - \mathbf{O}_{J,J}(\mathbf{q}) \tag{5.1b}$$

Then since

$$\tan 4\Theta = \frac{2\mathbf{O}_{I,J} \cdot \bar{\mathbf{G}}_{I,J}}{\mathbf{O}_{I,J} - \bar{\mathbf{G}}_{I,J} \cdot \bar{\mathbf{G}}_{I,J}}$$
(5.1c)

$$n(\mathbf{q}) = 2\bar{\mathbf{G}}_{I,J}(\mathbf{q}) \cdot \mathbf{O}_{I,J}(\mathbf{q}) \quad d(\mathbf{q}) = \mathbf{O}_{I,J} \cdot \mathbf{O}_{I,J} - \bar{\mathbf{G}}_{I,J} \cdot \bar{\mathbf{G}}_{I,J}$$
(5.1d)

for $I = 1^1 A$ and $J = 2^1 A$. Here $\mathbf{O}_{I,J}$ and $\bar{\mathbf{G}}_{I,J}$ are 3-component vectors.

The pathologies associated with DSPs are illustrated in Fig. $\bf 1$ which is relevant to the photodissociation reaction:

$$NH_3(\widetilde{X}^1A) + hv \rightarrow NH_3(\widetilde{A}^1A) \rightarrow NH_2(\widetilde{X}^2A) + H$$

Fig. 1 plots $||\mathbf{f}^{(a),1,2,(x)}||$ along a path leading from the D_{3h} minimum of the 2^1A state to the minimum energy CI of the $1,2^1A$ states of NH_3 . The x=BL determined norm is given by the gray line in Fig. 1. From this figure it is seen that the singularity in the *ab initio* determined derivative coupling (red circles, x=ab *initio*) is well reproduced near the CI at $R(N-H)=\sim 3.6$ a_0 , by the BL diabatization as expected. However, the BL determined derivative coupling presents a second singularity of $||\mathbf{f}^{(a),1,2,(BL)}||$ near R=2.4 a_0 where $||\mathbf{f}^{(a),1,2,(ab)}||$ is small, that is where the adiabatic states are well separated energetically. This is a diabolical singularity.

The remainder of the discussion in this section deals with locating the DSPs and for that reason we turn to the photodissociation of

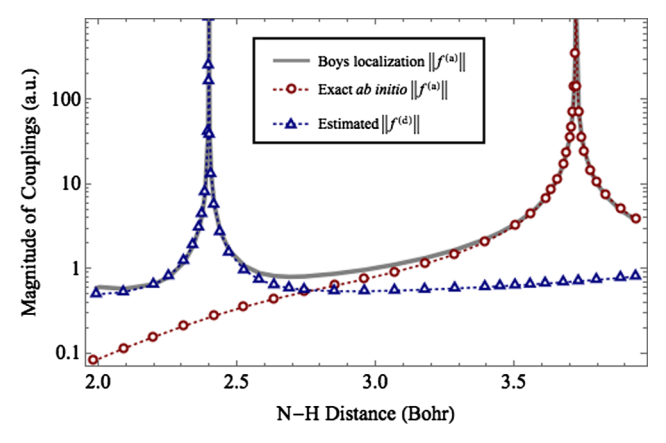


Fig. 1. Comparison of the norm of the derivative coupling obtained using BL approach diagonalization (gray line) with the exact ab initio determined $||f^{(a)}||$ (red open circles) along a path leading from the D_{3h} minimum for the 2^1A state to the minimum energy CI of the $1,2^1A$ states of NH₃. Also reported is an estimate of $||f^{(d)}||$ (blue triangles). From Ref. [60] with permission from the American Chemical Society.

Table 1 Energies at DSPs and equilibrium geometries. Norms of right hand side of Eq. (3.14), $\|\nabla L\|$, |d|, and |n|, a.b × 10^{c} written as a.b(c).

	DSP(1)	DSP(2)	$1^{1}A_{eq}$	2¹A _{eq}
E_1 E_2 $ \nabla L $ $ d $	7752 49,058 0.90(-2) 0.880(-5)	10,199 47,590 0.012 0.116(-5)	0 48,747	2991 43,589
a n	0.880(-5) 0.119(-5)	0.116(-5) 0.493(-7)		

methylamine:

$$\operatorname{CH}_3\operatorname{NH}_2(\widetilde{X}^1A) + hv \rightarrow \operatorname{CH}_3\operatorname{NH}_2(\widetilde{A}^1A) \rightarrow \operatorname{CH}_3\operatorname{NH}(\widetilde{X}^2A) + \operatorname{H} ; \operatorname{NH}_2(\widetilde{X}^2A) + \operatorname{CH}_3(\widetilde{X}^2A)$$

which has many more internal degrees of freedom. Illustrative of what can be done, Table 1 reports E_1 , E_2 , $||\nabla L_p||$, |n|, and |d| for two solutions of Eq. (3.14) with $M^c = 0$ and P = 1, 2 obtained using the Hessian approximation in Eq. (3.16).

The solution DSP(1) uses P = 1, that is, the ground state energy is minimized subject to the constraints. The solution DSP(2) uses P = 2. The iterative sequence for converging Eq. (3.14) for DSP(2) is reported in Table 2.

Note that at the starting point n and d are zero initially but $||\nabla L_2||$ is large. Correcting ∇L_2 causes n and d to deviate from zero but this is temporary and by iteration 4 convergence is approximately monotonic.

From Table 1, it is seen that following a vertical excitation from the equilibrium structure on the 1^1A state, 1^1A_{eq} , the point DSP(2) [DSP(1)] is [is almost] energetically accessible on 2^1A PES. In this regard note that the energy of DSP(2) falls into the first UV absorption band of methylamine [68]. The preceding observation demonstrates the importance of knowing both the energy and location of the seam of DSPs.

Table 2 Convergence of Eq. (3.14). DSP(2) Search. a.b \times 10^c written as a.b(c).

	n	d	$ L_2 $	E_1	E_2
0	0.806(-7)	-0.220(-6)	2.102	28951.5	60230.9
1	-0.242(-5)	0.480(-1)	0.824	16345.6	53668.7
2	0.134(-3)	0.182(-1)	0.623	9904.7	47884.1
3	0.172(-4)	0.586(-1)	0.347	9764.3	47551.2
4	-0.173(-5)	0.344(-1)	0.118	9071.2	46948.3
5	-0.183(-5)	0.344(-2)	0.061	10089.7	47545.0
6	0.427(-4)	0.136(-3)	0.034	10209.9	47602.1
7	-0.228(-6)	0.927(-5)	0.022	10207.1	47589.7
8	0.493(-7)	0.116(-5)	0.012	10199.6	47589.8

Once low energies DSPs have been located the diabatization scheme can be modified if needed.

5.2. Constructing accurate vector potentials: The 2,3¹A states of phenol

The two state representations discussed in Section 4 have several significant uses. As discussed in that section the removable adiabatic derivative couplings can be used to determine the GP/VP needed to make the corresponding adiabatic electronic wave functions single-valued. Consequently they can be, and have been, used to study nonadiabatic tunneling in the one state limit using Eq. (2.10) [69]. Further since the two state representation is a rigorously removable approximation it is unitarily equivalent to the diabatic representation except at the singular points (CIs). Therefore, nonadiabatic tunneling can be studied in the "exact" two state diabatic representation using Eq. (3.4). Comparing the two results provides insights into the mechanism of nonadiabatic tunneling. These descriptions can also be used to study the limitations of the one state adiabatic representation, Eq. (2.10) and the relations between the two state adiabatic and diabatic representations. Finally, since the diabatic representation is built from accurate ab initio data, energies, energy gradients and derivative couplings, it can be validated by comparison with experiments.

Recently, there has been considerable theoretical work on tunneling in phenol photodissociation [10,66,69–76]. Of particular relevance here are studies of nonadiabatic tunneling which suggest that including the MAB effect can change the predicted tunneling dissociation rate by well over an order of magnitude [10,66]. Furthermore, the MAB effect can lead to different product state distributions from those predicted by a single adiabatic state approximation [67].

There has been limited consideration of the MAB effect on classically allowed or tunneling reaction dynamics in real systems owing to technical issues: the lack of a computationally useful general formulation of the MAB Hamiltonian and a method of dealing with the singular terms in the MAB Hamiltonian. The methodology reviewed here addresses the first hurdle, namely the *ab initio* determination of the phase factor used to render the total wave function single-valued. This is accomplished in two steps. First the ZY diabatization is used to construct a removable approximation to *ab initio* data including adiabatic derivative couplings. This removable derivative coupling is then used as in Eqs. (2.9) and (4.1) to construct the GP needed to make an adiabatic electronic wave function single-valued.

The nuclear dynamics issues are associated with the convergence of integrals involving the DBOC. In general, the higher the total energy the more problematic the convergence of the DBOC integrals. Since in nonadiabatic tunneling the CI is energetically inaccessible, that is its energy is well above that of the total energy, it is a particularly favorable situation for our strategy.

Here, we review the numerical issues associated with the electronic structure aspects of this strategy. The electronic structure data we use is taken from a full 33-dimensional *ab initio* treatment of phenol photodissociation through its excited S_1 state:

$$C_6H_5OH(S_0) + hv \rightarrow C_6H_5OH(S_1,S_2) \rightarrow C_6H_5O + H$$

based on a ZY diabatization [54]. This nonadiabatic process has been the subject of much recent interest [77]. As seen in Fig. 2, there is a low-lying S_1 - S_2 CI and two, symmetrically displaced, lower-energy adiabatic saddle points on S_1 . This is the archetypical topography for nonadiabatic tunneling in dissociative dynamics on S_1 [66].

Two directly comparable coupled diabatic state representations are employed: a four-diabatic-state representation of (S_0, S_1, S_2, S_3) , $\mathbf{H}^{d,(4)}$, based on the original *ab initio* data and a two-diabatic-state representation of (S_1, S_2) $\mathbf{H}^{d,(2)}$ deduced from $\mathbf{H}^{d,(4)}$ adiabatic data. S_1 and S_2 are states 1 and 2 from $\mathbf{H}^{d,(2)}$ while they are states 2 and 3 from $\mathbf{H}^{d,(4)}$. The principal issue is that according to Appendix B, $\mathbf{f}^{(a),S_1,S_2,(m4)}$ obtained from $\mathbf{H}^{d,(4)}$ are non-removable while $\mathbf{f}^{(a),S_1,S_2,(m2)}$ obtained from $\mathbf{H}^{d,(2)}$ are removable. Our analysis will consider the following points: (a)

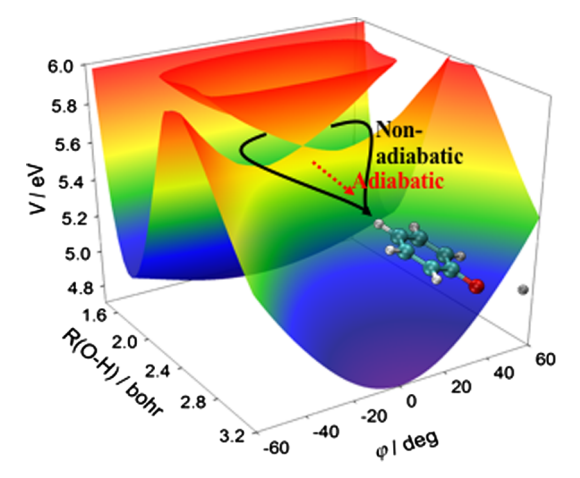


Fig. 2. S_1 and S_2 PES and their CI for phenol photodissociation, $C_6H_5OH + hv \rightarrow C_6H_5O + H$. Reproduced from Ref. [33] with permission from the PCCP Owner Societies.

the size and kind of error in the circulation of the $\mathbf{H}^{d,(w)}$ (w=2,4) determined derivative coupling $\mathbf{f}^{(a),S_1,S_2,(mw)}(\mathbf{R})$ along a circle in the *g-h* plane centered at $\mathbf{O} = (x^0, y^0, \mathbf{z}^0)$, with radius r;

$$C(w, \mathbf{O}, r) = \oint \mathbf{f}^{(a), S_1, S_2, (mw)}(\mathbf{R}') \cdot d\mathbf{R}'$$
(5.2)

(b) the accuracy of the numerical quadratures and how the numerical errors compare to the errors attributable to non-removability; and (c) how seam curvature which is omitted in simplified models of the GP effect is described. We note that the overall sign of the reported circulations depends on the sign of the initial $\mathbf{f}^{(a),S_1,S_2,(mx)}(\mathbf{R})$. Since this sign is irrelevant in the present context we only use it to improve the clarity of the figures that follow. Three classes of figures/paths are reviewed: (a) circles with the minimum energy S_1 - S_2 CI at the origin (Fig. 3); (b) circles with the origin displaced (Fig. 4) and (c) figures describing seam curvature (Fig. 5).

(a) Path 1 = Circles centered at the origin

Fig. 3 juxtaposes the $\mathbf{H}^{d,(2)}$ and $\mathbf{H}^{d,(4)}$ determined energies and derivative couplings at the indicated r. Note the good agreement between the $\mathbf{H}^{d,(4)}$ and $\mathbf{H}^{d,(2)}$ determined energies for r=0.2 and 0.5. The results for r = 0.2 are typical of the r < 0.2 results. For C(2, (0,0,0), r) the integral consists of two identical halves which add to give π exact to 8 decimal places. This indicates the quality of $f_{\theta}^{(a),S_1,S_2,(m2)}(\rho,\theta)$ and that a single CI (at the origin) is enclosed in the loop. The accuracy of these circulations strongly supports the utility of this approach. For $C(4,(0,0,0), r \le 0.2)$, the contribution of the non-removable part of $f_{\rho}^{(a),S_1,S_2,(m4)}(\rho,\theta)$ is quite small and although it does increase with increasing r, probably could be tolerated in numerical calculations. For the larger radius, r = 0.5, C(4,(0,0,0), r=0.5), differs significantly from π , suggesting a large nonremovable part. However, this is contraindicated by satisfactory agreement of $f_{\beta}^{(a),S_1,S_2,(mx)}(\rho,\theta)$, for x=2 and x=4 evinced in Fig. 3b. Section 5.3 explains this ruinous discrepancy.

(b) Path 2 = Circles centered away from the origin

For the frequently used linear vibronic coupling model [78], the CI seam is a single (generalized) single straight line. However, when quadratic terms are included, additional seams of CIs can exist which intersect the g-h planes [79,80]. To consider this situation, the center of the circle is repositioned so that the CIs do not occur at the circle's center. This can give rise to the type of circulation illustrated in Fig. 4(b-c), which consider $\mathbf{H}^{d,(2)}$ and $\mathbf{H}^{d,(4)}$ determined circulations for loops pictured in Fig. (4a). In these figures the origin is not a CI. The CI is located at the intersection of the vertical and horizontal lines. Thus, for w = 2, $C(w,(t^s,t^s,0),r) = 0$ for $r < t^s \sqrt{2}$ (Fig. (4b)) and $C(w,t^s,t^s,0)$ $(t^s, t^s, \mathbf{0}), r) = \pi$ for $r > t^s \sqrt{2}$ (Fig. (4c)). The derivative couplings change rapidly in the vicinity of the CI indicating the need for care in carrying out integrals involving the derivative coupling.

(c) Path $3 = Seam \ curvature$

Up to this point, we have considered single points of CIs without regard to their connectivity. Seam curvature, the fact that for $z \neq 0$ CIs do not occur at (x,y) = (0,0), is illustrated in Fig. 5. Plate (5a) shows the $\mathbf{H}^{d,(2)}$ and $\mathbf{H}^{d,(4)}$ determined seams, the black lines, determined as a function of $R(CO) \sim z_2$. Loops used to evaluate circulations C(w, v) $(0,0,z_2)$, r) are shown for fixed values of z in planes parallel to the g-h plane for z = 0. Near $\mathbf{z} = 0$ $C(w,(0,0,z_2),r) = \pi$ for all r used as the CI at (x,y,z) is close to (0,0,z). However, as |z| increases the $\rho = (x^2 + y^2)^{1/2}$ for which the CI is first enclosed increases. For $r < \rho$, C(w, v) $(0,0,z_2),r)=0$ since no CI is contained in the loop. Increasing r eventually encloses the CI and $C(w,(0,0,z_2),r)$ becomes π . Here, it is important to note that the only computed values of $C(2,(0,0,z_2),r)$ are 0 or π . Similar, but not identical, results are obtained for w = 4, indicating that the non-removable contribution is small.

The 2-state diabatic Hamiltonian was used in a three-dimensional quantum dynamics study and it was shown that the wave function node closely tracks the CI seam, illustrating the dynamic mapping of the CI

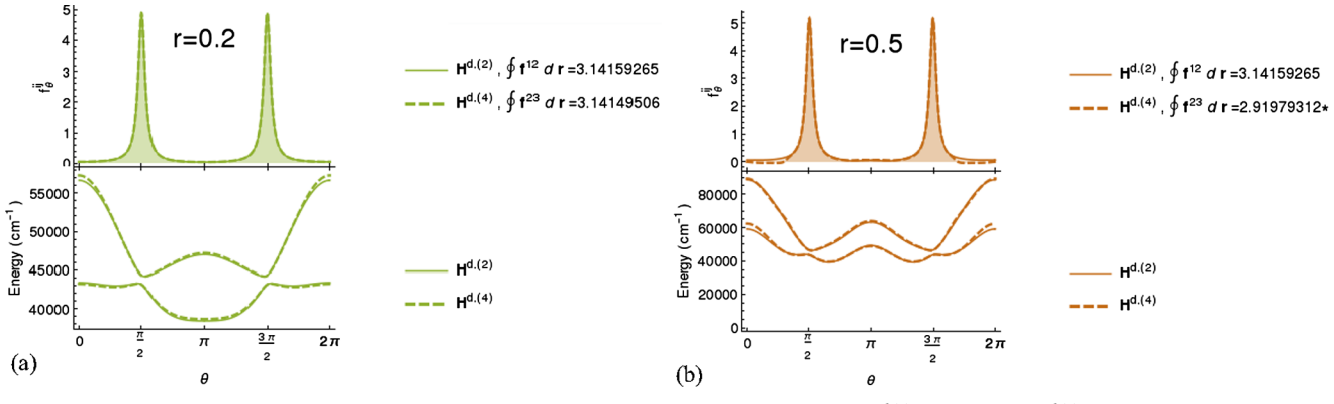


Fig. 3. Derivative couplings and circulations (upper panels), S_1 and S_2 energies (lower panels). Solid lines: $\mathbf{H}^{d,(2)}$, dashed lines: $\mathbf{H}^{d,(4)}$ determined quantities. From Ref. [27] with permission of AIP.

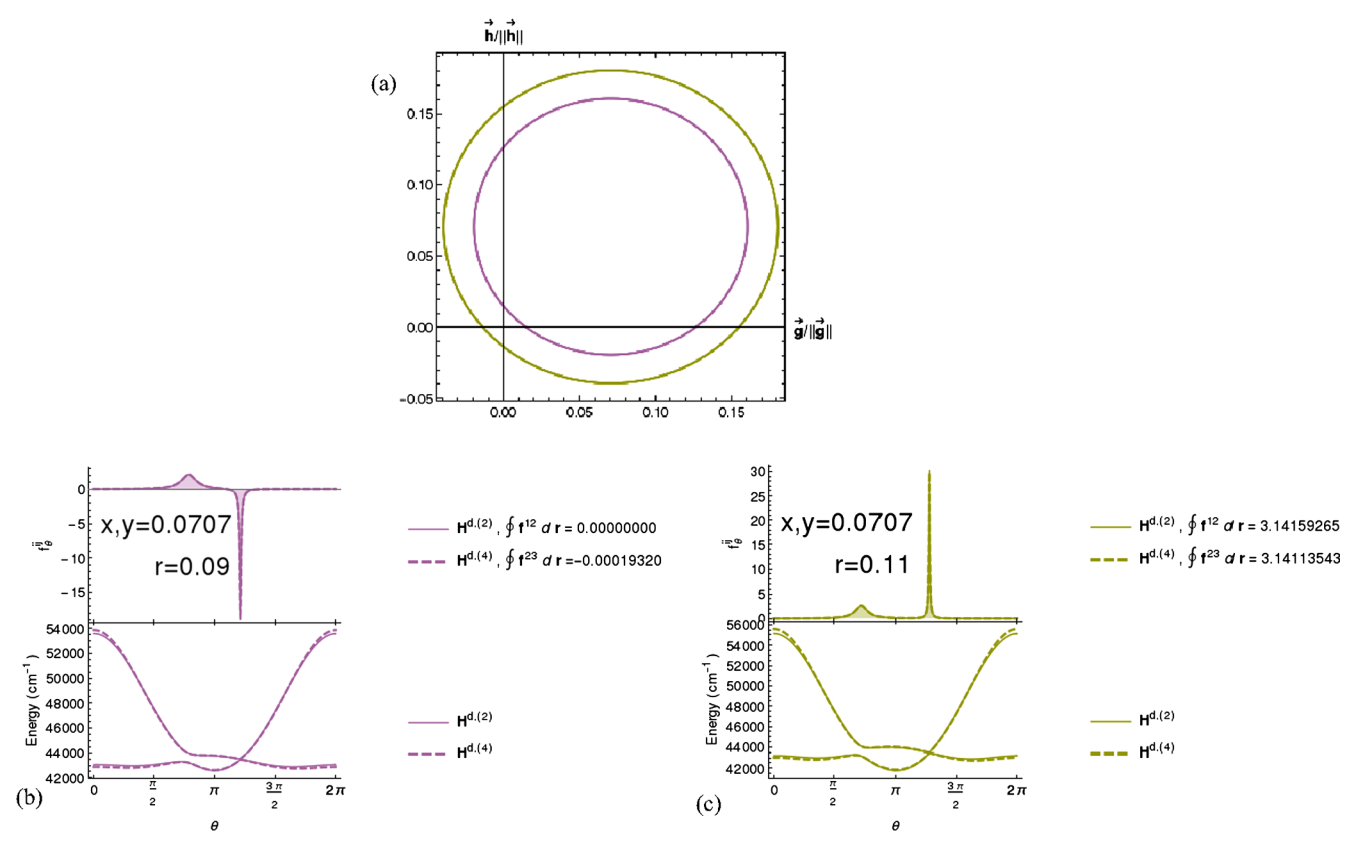


Fig. 4. (a) Loops used in panel (b) (inner) and (c) (outer) respectively. Panels (b) and (c) derivative couplings and circulations (upper panels), S_1 and S_2 energies (lower panels). Solid lines $\mathbf{H}^{d,(2)}$, dashed lines $\mathbf{H}^{d,(4)}$ determined quantities. From Ref. [27] with permission of AIP.

5.3. Linked conical intersections

This concluding section addresses the treatment of nonadiabatic dynamics in the coupled adiabatic state representation for more than two states. To treat more than two electronic states, it is seen from Eq. (2.8) that the derivative couplings $\mathbf{f}^{(a),J,K,(x)}(\mathbf{R})$ (x = m or ab) will be required. Consider, by way of example, the four coupled-adiabatic-state description of phenol based on $\mathbf{H}^{d,(4)}$ described in Section 5.2. The line integrals discussed in Section 5.2 reveal the issue. For origin centered circulations of $\mathbf{f}^{(a),2,3,(m4)}(\mathbf{R})$ based on $\mathbf{H}^{d,(4)}$, the non-removable contribution increases with increasing r. This reflects an increase in the derivative coupling between states 3 and 4 as their separation decreases. When states 3 and 4 intersect conically for $r = \sim 0.26$ the circulation changes abruptly and dramatically. The existence of a CI of states 3 and 4 for $r = \sim 0.26$ renders $\mathbf{f}^{(a),2,3,(m4)}(\rho = 0.3, \theta)$ double-valued, since now state 3 does not change sign on traversing the loop but state 2 does. For r > 0.58 a second 3-4 CI exists. So for loops with r > 0.58 state 2 (3) is transported along a loop containing 1 (3) CIs. Thus, both states change sign and $\mathbf{f}^{(a),2,3,(m4)}(\rho = 0.59, \theta)$ is single-valued. The situation is reflected in the circulations reported in Table 3, for a series of starting angles, $\theta = \phi$, and r = 0.25, 0.30 and 0.59. For r = 0.3 (actually any r with 0.26 < r < 0.59 will work) the circulation is starting point, choice of ϕ , dependent.

These results are completely consistent with the formal analysis in Ref. [34], by Han and Yarkony (HY). CIs of states 2,3 and 3,4 are referred to as linked CIs by HY. HY show that for linked CIs of states I, J, K, the I, J circulation depends on the starting point. Further the circulation from 0 to 4π is zero rather than twice the integral from 0 to 2π as would be expected. This pathology is not evident from a single construction of the circulation. However, the starting point dependence of

the circulation (requiring two evaluations of the circulation) or integrating to 4π can be used to detect this situation.

When this arrangement of CIs exists, since $\mathbf{f}^{(a),I,J}$ will be double-valued, there is no consistent way to formulate Eqs. (2.7) or (2.8), i.e., use the coupled adiabatic state representation.

6. Summary

In this Viewpoint issues in the construction and use of adiabatic and diabatic representations in nonadiabatic electronic structure/dynamics are described. Three fundamental issues are reviewed.

(i) The construction of the AtD transformation based on representations of smooth molecular properties, (more generally a vector of Hermitian operators) can be compromised by the existence of diabolical singular points a space of dimension $N^{int}-2$ where the AtD transformation is singular. The space of diabolical singular points has the same dimension as the seam of conical intersection, but is different. This singularity produces fallacious singularities in the derivative coupling. A procedure is reviewed in Section 3.4 and illustrated in Section 5.1 that can locate energetically relevant singularities in the AtD transformation. In future work the prevalence of these fallacious singularities will be accessed and extensions to $N^{\rm state}>2$ developed.

The remaining two topics deal with properties of the derivative couplings, $\mathbf{f}^{I,J}(\mathbf{R})$.

(ii) As reviewed in Sections 4 and 5.2, for $N^{\text{state}} = 2$ the $f^{I,J}(\mathbf{R})$ obtained from an (accurate) diabatization (for example a ZY diabatization of accurate *ab initio* data) enable the construction of a rigorous vibronic wave function based on adiabatic electronic states which properly accounts for the GP. This formulation introduces a rigorous VP into the nuclear Schrödinger equation making this adiabatic states based

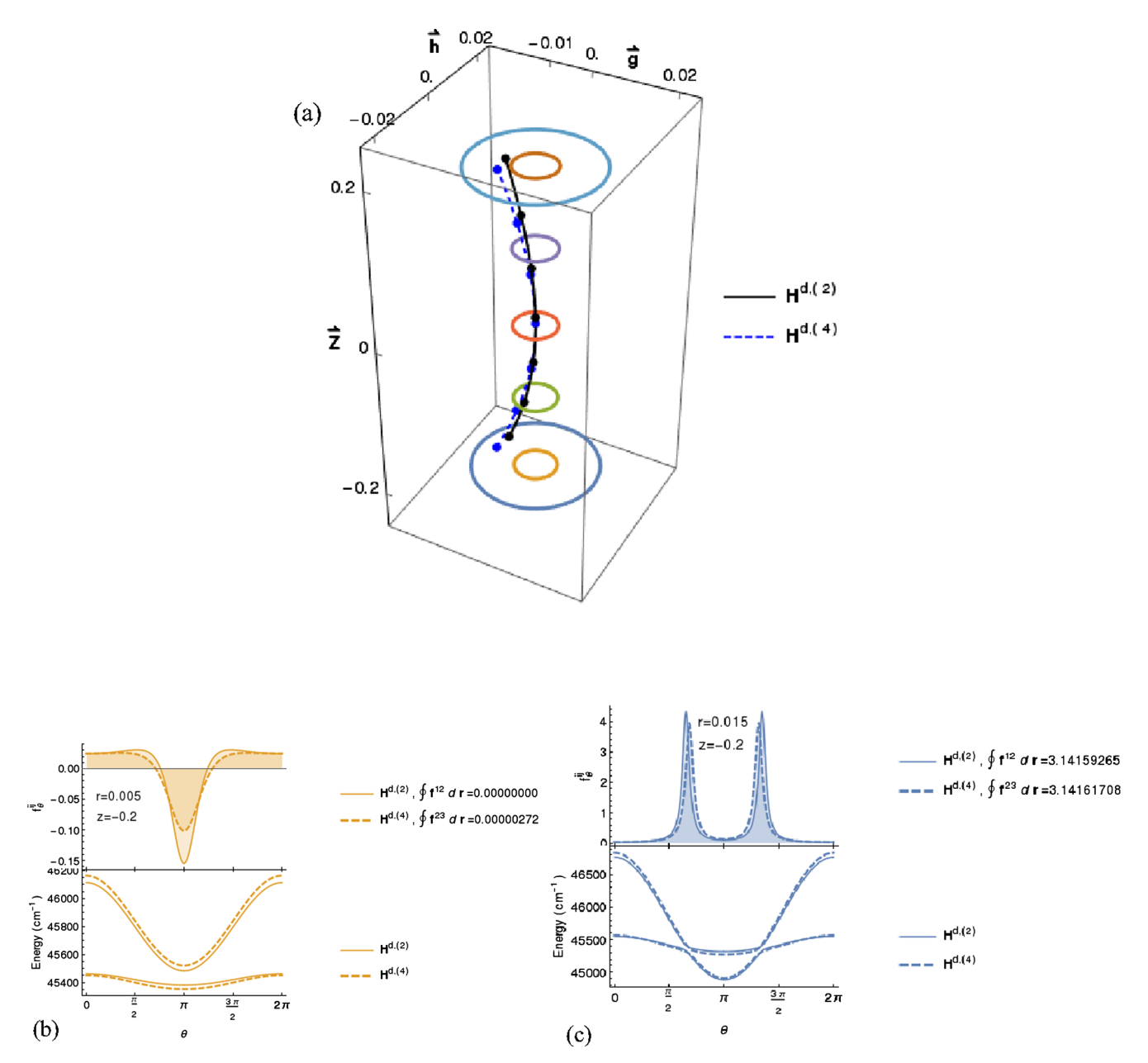


Fig. 5. Seam curvature. (a) Loops in the g-h plane displaced along a z_i -axis demonstrating the effect of seam curvature along the z_i direction on the circulation. Panels (b) and (c) respectively for z = -0.2, r = 0.005 and 0.015. Derivative couplings and circulations found in upper panels, S_1 and S_2 energies in lower panels. Solid lines $\mathbf{H}^{d,(2)}$, dashed lines $\mathbf{H}^{d,(4)}$ determined quantities. From Ref. [27] with permission of AIP.

Table 3 $C(4, (0, 0, \mathbf{0}), r)$ as a function of ϕ for three values of r.

$\phi(\deg)$	C(4, (0, 0, 0), r)					
	r = 0.25	r = 0.3	r = 0.59			
0	3.13654714	3.06439078	2.85767507			
30	3.13654714	3.07245028	2.85767507			
60	3.13654714	2.96704120	2.8576750			
90	3.13654714	-1.60163491	2.85767507			
120	3.13654714	-0.15961872	2.85767507			
150	3.13654714	-0.05023925	2.85767507			
180	3.13654714	0.00000000	2.85767507			
210	3.13654714	0.05023925	2.85767507			
240	3.13654714	0.15961872	2.85767507			
270	3.13654714	1.60163491	2.8576750			
300	3.13654714	-2.96704120	2.8576750			
330	3.13654714	-3.07245028	2.85767507			

nuclear Schrödinger equation, when solvable, rigorously equivalent to the results in the diabatic representation.

(iii) The $\mathbf{f}^{I,J}(\mathbf{R})$ arise naturally as coupling the adiabatic electronic states in nonadiabatic dynamics. When $N^{\text{state}} \geq 3$ (states denoted I, J, K, \ldots) $\mathbf{f}^{I,J}(\mathbf{R})$ and $\mathbf{f}^{J,K}(\mathbf{R})$, can become linked, that is paths exist which contain a CI of states (I,J) and of states (J,K). In this case $\mathbf{f}^{I,J}(\mathbf{R})$ and $\mathbf{f}^{J,K}(\mathbf{R})$ become double valued and are not suitable for nuclear dynamics since specifying \mathbf{R} should yield a unique value for $\mathbf{f}^{I,J}(\mathbf{R})$. The starting point dependence of the circulation of $\mathbf{f}^{I,J}(\mathbf{R})$ demonstrated in Section 5.3 was suggested as a way to determine the existence of this problem. In future work the magnitude of this problem, which complicates the use of the adiabatic representation, will be studied.

Funding

This work was supported by Department of Energy grant DE-SC0015997 (to H.G. and D.R.Y.) and National Science Foundation grant CHE-1663692 (to D.R.Y.).

Conflict of interest

The authors declare no competing financial interest.

Appendix A. Adiabatic to diabatic states (AtD) transformation

The off-diagonal derivative couplings in the diabatic representation are defined to be 0, that is

$$0 = \langle \Psi_{\alpha}^{(d)}(\mathbf{r}; \mathbf{R}) | \frac{\partial}{\partial R_k} \Psi_{\beta}^{(d)}(\mathbf{r}; \mathbf{R}) \rangle_{\mathbf{r}} \text{ for all } (\alpha, \beta) \text{ and } k.$$
(A.1)

Inserting the AtD transform Eq. (3.1a) into Eq. (A.1) gives

$$= < \sum_{K} U_{K,\alpha} \Psi_{K}^{(a)} | \nabla \sum_{K'} U_{K',\beta} \Psi_{K'}^{(a)} > = < \sum_{K} U_{K,\alpha} \Psi_{K}^{(a)} | \sum_{K'} \nabla U_{K',\beta} \Psi_{K'}^{(a)} + \sum_{K'} U_{K',\beta} \nabla \Psi_{K'}^{(a)} >$$
(A.2)

$$= \sum_K U_{K,\alpha} \nabla U_{K,\beta} + \sum_{K,K'} U_{K,\alpha} U_{K',\beta} < \Psi_K^{(a)} | \nabla \Psi_{K'}^{(a)} >$$

$$= \sum_{K} U_{K,\alpha} \nabla U_{K,\beta} + \sum_{K,K'} U_{K,\alpha} \mathbf{f}^{K,K'} U_{K',\beta}$$
(A.3)

Then, multiplying both sides by $U_{L,\alpha}$ and summing on α gives

$$\sum_{K,\alpha} U_{L,\alpha} U_{K,\alpha} \nabla U_{K,\beta} + \sum_{K,\alpha,K'} U_{L,\alpha} U_{K',\beta} U_{K,\alpha} \mathbf{f}^{K,K'}$$
(A.4)

$$0 = \nabla U_{L,\beta} + \sum_{K'} \mathbf{f}^{L,K'} U_{K',\beta} \tag{A.5}$$

So

$$\nabla \mathbf{U} + \mathbf{f} \mathbf{U} = \mathbf{0} \tag{A.6}$$

Appendix B. The curl condition [29,36]

Starting from Eq. (A.6) and defining $p = R_p$ and $q = R_q$

$$\frac{\partial}{\partial q} \frac{\partial}{\partial p} U_{L,\alpha} - \frac{\partial}{\partial p} \frac{\partial}{\partial q} U_{L,\alpha} =$$

$$-\left\{\frac{\partial}{\partial q}\sum_{K=1}^{N}f_{p}^{L,K}U_{K,\alpha}-\frac{\partial}{\partial p}\sum_{K=1}^{N}f_{q}^{L,K}U_{K,\alpha}\right\}$$
(B.1)

$$= -\left\{ \sum_{K=1}^{N} \left(\frac{\partial}{\partial q} f_p^{L,K} U_{K,\alpha} + f_p^{L,K} \frac{\partial}{\partial q} U_{K,\alpha} - \frac{\partial}{\partial p} f_q^{L,K} U_{K,\alpha} - f_q^{L,K} \frac{\partial}{\partial p} U_{K,\alpha} \right) \right\}$$
(B.2)

$$= - \left\{ \sum_{K=1}^{N} \left(\frac{\partial}{\partial q} f_{p}^{L,K} U_{K,\alpha} - f_{p}^{L,K} \sum_{K'=1}^{N} f_{q}^{K,K'} U_{K',\alpha} - \frac{\partial}{\partial p} f_{q}^{L,K} U_{K,\alpha} \right) + f_{q}^{L,K} \sum_{K'=1}^{N} f_{p}^{K,K'} U_{K',\alpha} \right\}$$
(B.3)

$$= -\left\{ \sum_{K=1}^{N} \left(\frac{\partial}{\partial q} f_{p}^{L,K} U_{K,\alpha} - \frac{\partial}{\partial p} f_{q}^{L,K} U_{K,\alpha} - f_{p}^{L,K} \sum_{K'=1}^{N} f_{q}^{K,K'} U_{K',\alpha} \right) + f_{q}^{L,K} \sum_{K'=1}^{N} f_{p}^{K,K'} U_{K',\alpha} \right\}$$
(B.4)

then factoring out U from the right, Eq. (B.4) in matrix form is

$$= -\left[\left\{ \frac{\partial}{\partial q} \mathbf{f}_p - \frac{\partial}{\partial p} \mathbf{f}_q - \mathbf{f}_p \mathbf{f}_q + \mathbf{f}_q \mathbf{f}_p \right\} \mathbf{U} \right]_{L,\alpha}$$
(B.5)

So the mixed partial derivatives are equal, provided $N^{state} = N^{es}$ since

$$\left\{ \frac{\partial}{\partial q} \mathbf{f}_p - \frac{\partial}{\partial p} \mathbf{f}_q + \mathbf{f}_p \mathbf{f}_q - \mathbf{f}_q \mathbf{f}_p \right\}_{K,L} = \sum_{M=N^{\text{State}}+1}^{N^{\text{es}}} (f_p^{M,K} f_q^{M,L} - f_q^{M,K} f_p^{M,L}) = 0$$
(B.6)

References

- [1] M. Born, K. Huang, Dynamical Theory of Crystal Lattices, Clarendon, Oxford, 1954.
- [2] M. Born, R. Oppenheimer, Quantum theory of molecules, Ann. Phys. 84 (1927) 0457–0484.
- [3] H.C. Longuet-Higgins, U. Öpik, M.H.L. Pryce, R.A. Sack, Studies of the Jahn-Teller effect. II. The dynamical problem, Proc. Royal Soc. A (London) 244 (1958) 1–16.
- [4] C.A. Mead, D.G. Truhlar, On the determination of Born-Oppenheimer nuclear motion wave functions including complications due to conical intersections and identical nuclei, J. Chem. Phys. 70 (1979) 2284–2296.
- [5] M.V. Berry, Quantal phase factors accompanying adiabatic changes, Proc. Royal Soc. A (London) 392 (1984) 45–57.
- [6] N.C. Handy, Y. Yamaguchi, H.F. Schaefer, The diagonal correction to the Born-Oppenheimer approximation: Its effect on the singlet-triplet splitting of CH₂ and other molecular effects, J. Chem. Phys. 84 (1986) 4481–4484.

- [7] R. Gherib, L. Ye, I.G. Ryabinkin, A.F. Izmaylov, On the inclusion of the diagonal Born-Oppenheimer correction in surface hopping methods, J. Chem. Phys. 144 (2016) 154103.
- [8] J.C. Tully, Molecular dynamics with electronic transitions, J. Chem. Phys. 93 (1990) 1061–1071.
- [9] I.G. Ryabinkin, A.F. Izmaylov, Geometric phase effects in dynamics near conical intersections: Symmetry breaking and spatial localization, Phys. Rev. Lett. 111 (2013) 220406.
- [10] C. Xie, D.R. Yarkony, H. Guo, Nonadiabatic tunneling via conical intersections and the role of the geometric phase, Phys. Rev. A 95 (2017) 022104.
- [11] L. Joubert-Doriol, I.G. Ryabinkin, A.F. Izmaylov, Geometric phase effects in low-energy dynamics near conical intersections: A study of the multidimensional linear vibronic coupling model, J. Chem. Phys. 139 (2013) 234103.
- [12] I.G. Ryabinkin, L. Joubert-Doriol, A.F. Izmaylov, When do we need to account for the geometric phase in excited state dynamics? J. Chem. Phys. 140 (2014) 214116.
- [13] R. Gherib, I.G. Ryabinkin, A.F. Izmaylov, Why do mixed quantum-classical methods describe short-time dynamics through conical intersections so well? Analysis of geometric phase effects, J. Chem. Theo. Comput. 11 (2015) 1375–1382.
- [14] B. Kendrick, R.T. Pack, Geometric phase effects in H+O₂ scattering. I. Surface function solutions in the presence of a conical intersection, J. Chem. Phys. 104 (1996) 7475–7501.
- [15] B. Kendrick, R.T. Pack, Geometric phase effects in H+O₂ scattering. II. Recombination resonances and state-to-state transition probabilities at thermal energies, J. Chem. Phys. 104 (1996) 7502–7514.
- [16] B.K. Kendrick, Geometric phase effects in chemical reaction dynamics and molecular spectra, J. Phys. Chem. A 107 (2003) 6739–6756.
- [17] B.K. Kendrick, J. Hazra, N. Balakrishnan, Geometric phase appears in the ultracold hydrogen exchange reaction, Phys. Rev. Lett. 115 (2015) 153201.
- [18] B.K. Kendrick, J. Hazra, N. Balakrishnan, The geometric phase controls ultracold chemistry, Nat. Commun. 6 (2015) 7918.
- [19] J.C. Juanes-Marcos, S.C. Althorpe, Geometric phase effects in the H+H₂ reaction: Quantum wave-packet calculations of integral and differential cross sections, J. Chem. Phys. 122 (2005) 204324.
- [20] J.C. Juanes-Marcos, S.C. Althorpe, E. Wrede, Theoretical study of geometric phase effects in the hydrogen-exchange reaction, Science 309 (2005) 1227–1230.
- [21] S.C. Althorpe, General explanation of geometric phase effects in reactive systems: Unwinding the nuclear wave function using simple topology, J. Chem. Phys. 124 (2006) 084105.
- [22] S.C. Althorpe, T. Stecher, F. Bouakline, Effect of the geometric phase on nuclear dynamics at a conical intersection: Extension of a recent topological approach from one to two coupled surfaces, J. Chem. Phys. 129 (2008) 214117.
- [23] F. Bouakline, S.C. Althorpe, D. Peláez Ruiz, Strong geometric-phase effects in the hydrogen-exchange reaction at high collision energies, J. Chem. Phys. 128 (2008) 124322.
- [24] C.A. Mead, The molecular Aharonov—Bohm effect in bound states, Chem. Phys. 49 (1980) 23–32.
- [25] Y. Aharonov, D. Bohm, Significance of electromagnetic potentials in the quantum theory, Phys. Rev. 115 (1959) 485–491.
- [26] P.W. Foster, D.M. Jonas, Nonadiabatic eigenfunctions can have amplitude, signed conical nodes, or signed higher order nodes at a conical intersection with circular symmetry, J. Phys. Chem. A 121 (2017) 7401–7413.
- [27] C.L. Malbon, X. Zhu, H. Guo, D.R. Yarkony, On the incorporation of the geometric phase in general single potential energy surface dynamics: A removable approximation to ab initio data, J. Chem. Phys. 145 (2016) 234111.
- [28] M. Baer, Adiabatic and diabatic representations for atom-diatom collisions: Treatment of the three-dimensional case, Chem. Phys. 15 (1976) 49–57.
- [29] C.A. Mead, D.G. Truhlar, Conditions for the definition of a strictly diabatic electronic basis for molecular systems, J. Chem. Phys. 77 (1982) 6090–6098.
- [30] M. Baer, Introduction to the theory of electronic non-adiabatic coupling terms in molecular systems, Phys. Rep. 358 (2002) 75–142.
- [31] C.A. Mead, Electronic Hamiltonian, wave functions, and energies, and derivative coupling between Born-Oppenheimer states in the vicinity of a conical intersection, J. Chem. Phys. 78 (1983) 807–814.
- [32] G.A. Meek, B.G. Levine, Wave function continuity and the diagonal Born-Oppenheimer correction at conical intersections, J. Chem. Phys. 144 (2016) 184109.
- [33] H. Guo, D.R. Yarkony, Accurate nonadiabatic dynamics, Phys. Chem. Chem. Phys. 18 (2016) 26335–26352.
- [34] S. Han, D.R. Yarkony, Nonadiabatic processes involving three electronic states. I. Branch cuts and linked pairs of conical intersections, J. Chem. Phys. 119 (2003) 5058–5068.
- [35] Z.H. Top, M. Baer, Incorporation of electronically nonadiabatic effects into bimolecular reactive systems. I. Theory, J. Chem. Phys. 66 (1977) 1363–1371.
- [36] M. Baer, Beyond Born-Oppenheimer: Electronic Nonadiabatic Coupling Terms and Conical Intersections, Wiley, New Jersey, 2006.
- [37] G.J. Atchity, K. Ruedenberg, Determination of diabatic states through enforcement of configurational uniformity, Theo. Chem. Acc. 97 (1997) 47–58.
- [38] H. Nakamura, D.G. Truhlar, Direct diabatization of electronic states by the fourfold way. II. Dynamical correlation and rearrangement processes, J. Chem. Phys. 117 (2002) 5576–5593.
- [39] H. Nakamura, D.G. Truhlar, Extension of the fourfold way for calculation of global diabatic potential energy surfaces of complex, multiarrangement, non-Born-Oppenheimer systems: Application to HNCO(S₀, S₁), J. Chem. Phys. 118 (2003) 6816–6829.
- [40] K.R. Yang, X. Xu, D.G. Truhlar, Direct diabatization of electronic states by the fourfold-way: Including dynamical correlation by multi-configuration

- quasidegenerate perturbation theory with complete active space self-consistent-field diabatic molecular orbitals, Chem. Phys. Lett. 573 (2013) 84–89.
- [41] X. Xu, K.R. Yang, D.G. Truhlar, Diabatic molecular orbitals, potential energies, and potential energy surface couplings by the 4-fold way for photodissociation of phenol, J. Chem. Theo. Comput. 9 (2013) 3612–3625.
- [42] H.J. Werner, W. Meyer, MCSCF study of the avoided curve crossing of the two lowest $^1\Sigma^+$ states of LiF, J. Chem. Phys. 74 (1981) 5802–5807.
- [43] R.J. Cave, M.D. Newton, Generalization of the Mulliken-Hush treatment for the calculation of electron transfer matrix elements, Chem. Phys. Lett. 249 (1996) 15–19
- [44] J.E. Subotnik, S. Yeganeh, R.J. Cave, M.A. Ratner, Constructing diabatic states from adiabatic states: Extending generalized Mulliken-Hush to multiple charge centers with Boys localization, J. Chem. Phys. 129 (2008) 244101.
- [45] S. Fatehi, E. Alguire, J.E. Subotnik, Derivative couplings and analytic gradients for diabatic states, with an implementation for Boys-localized configuration-interaction singles, J. Chem. Phys. 139 (2013) 124112.
- [46] C.R. Evenhuis, X. Lin, D.H. Zhang, D. Yarkony, M.A. Collins, Interpolation of diabatic potential-energy surfaces: Quantum dynamics on ab initio surfaces, J. Chem. Phys. 123 (2005) 134110.
- [47] X. Zhu, D.R. Yarkony, On the elimination of the electronic structure bottleneck in on the fly nonadiabatic dynamics for small to moderate sized (10-15 atom) molecules using fit diabatic representations based solely on ab initio electronic structure data: The photodissociation of phenol, J. Chem. Phys. 144 (2016) 024105.
- [48] T. Pacher, L.S. Cederbaum, H. Köppel, Approximately diabatic states from block diagonalization of the electronic Hamiltonian, J. Chem. Phys. 89 (1988) 7367–7381.
- [49] R.J. Cave, J.F. Stanton, Block diagonalization of the equation-of-motion coupled cluster effective Hamiltonian: Treatment of diabatic potential constants and triple excitations, J. Chem. Phys. 140 (2014) 214112.
- [50] H. Köppel, B. Schubert, The concept of regularized diabatic states for a general conical intersection, Mol. Phys. 104 (2006) 1069–1079.
- [51] V.C. Mota, A.J.C. Varandas, HN₂(²A') electronic manifold. II. Ab initio based double-sheeted DMBE potential energy surface via a global diabatization angle, J. Phys. Chem. A 112 (2008) 3768–3786.
- [52] W. Eisfeld, A. Viel, Higher order (A+E)⊗e pseudo-Jahn-Teller coupling, J. Chem. Phys. 122 (2005) 204317.
- [53] A. Viel, W. Eisfeld, Effects of higher order Jahn-Teller coupling on the nuclear dynamics, J. Chem. Phys. 120 (2004) 4603–4613.
- [54] X. Zhu, D.R. Yarkony, Fitting coupled potential energy surfaces for large systems: Method and construction of a 3-state representation for phenol photodissociation in the full 33 internal degrees of freedom using multireference configuration interaction determined data, J. Chem. Phys. 140 (2014) 024112.
- [55] C.E. Hoyer, X. Xu, D. Ma, L. Gagliardi, D.G. Truhlar, Diabatization based on the dipole and quadrupole: The DQ method, J. Chem. Phys. 141 (2014) 114104.
- [56] C.E. Hoyer, K. Parker, L. Gagliardi, D.G. Truhlar, The DQ and DQΦ electronic structure diabatization methods: Validation for general applications, J. Chem. Phys. 144 (2016) 194101.
- [57] X. Zhu, D.R. Yarkony, On the representation of coupled adiabatic potential energy surfaces using quasi-diabatic Hamiltonians: A distributed origins expansion approach, J. Chem. Phys. 136 (2012) 174110.
- [58] X. Zhu, D.R. Yarkony, Quasi-diabatic representations of adiabatic potential energy surfaces coupled by conical intersections including bond breaking: A more general construction procedure and an analysis of the diabatic representation, J. Chem. Phys. 137 (2012) 22A511.
- [59] X. Zhu, D.R. Yarkony, Constructing diabatic representations using adiabatic and approximate diabatic data – Coping with diabolical singularities, J. Chem. Phys. 144 (2016) 044104.
- [60] X. Zhu, D.R. Yarkony, On the construction of property based diabatizations: Diabolical singular points, J. Phys. Chem. A 119 (2015) 12383–12391.
- [61] Y. Wang, D.R. Yarkony, Determining whether diabolical singularities limit the accuracy of molecular property based diabatic representations: The 1,21A states of methylamine, J. Chem. Phys. 149 (2018) 154108.
- [62] C.A. Mead, Superposition of reactive and nonreactive scattering amplitudes in the presence of a conical intersection, J. Chem. Phys. 72 (1980) 3839–3840.
- [63] T.C. Thompson, G. Izmirlian, S.J. Lemon, D.G. Truhlar, C.A. Mead, Consistent analytic representation of the two lowest potential energy surfaces for Li₃, Na₃, and K₃, J. Chem. Phys. 82 (1985) 5597–5603.
- [64] A. Kuppermann, The Geometric Phase in Reaction Dynamics, in: R.E. Wyatt, J.Z.H. Zhang (Eds.), Dynamics of Molecules and Chemical Reactions, Marcel Dekker, New York, 1996, pp. 411–472.
- [65] C. Xie, C.L. Malbon, H. Guo, D.R. Yarkony, Up to a sign. The insidious effects of energetically Inaccessible conical intersections on unimolecular reactions, Acc. Chem. Res. 52 (2019) 501–509, https://doi.org/10.1021/acs.accounts.8b00571.
- [66] C. Xie, J. Ma, X. Zhu, D.R. Yarkony, D. Xie, H. Guo, Nonadiabatic tunneling in photodissociation of phenol, J. Am. Chem. Soc. 138 (2016) 7828–7831.
- [67] C. Xie, C.L. Malbon, D.R. Yarkony, D. Xie, H. Guo, Signatures of a conical intersection in adiabatic dissociation on the ground electronic state, J. Am. Chem. Soc. 140 (2018) 1986–1989.
- [68] G.C.G. Waschewsky, D.C. Kitchen, P.W. Browning, L.J. Butler, Competing bond fission and molecular elimination channels in the photodissociation of CH₂NH₂ at 222 nm, J. Phys. Chem. 99 (1995) 2635–2645.
- [69] C. Xie, C.L. Malbon, D.R. Yarkony, H. Guo, Dynamic mapping of conical intersection seams: A general method for incorporating the geometric phase in adiabatic dynamics in polyatomic systems, J. Chem. Phys. 147 (2017) 044109.
- [70] Z. Lan, W. Domcke, V. Vallet, A.L. Sobolewski, S. Mahapatra, Time-dependent quantum wave-packet description of the $^1\pi\sigma^*$ photochemistry of phenol, J. Chem.

- Phys. 122 (2005) 224315.
- [71] R.N. Dixon, T.A.A. Oliver, M.N.R. Ashfold, Tunnelling under a conical intersection: Application to the product vibrational state distributions in the UV photodissociation of phenols, J. Chem. Phys. 134 (2011) 194303.
- [72] H. An, K.K. Baeck, Quantum wave packet propagation study of the photochemistry of phenol: Isotope effects (Ph-OD) and the direct excitation to the $^1\pi\sigma^*$ state, J. Phys. Chem. A 115 (2011) 13309–13315.
- [73] X. Xu, J.J. Zheng, K.R. Yang, D.G. Truhlar, Photodissociation dynamics of phenol: Multi-state trajectory simulations including tunneling, J. Am. Chem. Soc. 136 (2014) 16378–16386.
- [74] K.R. Yang, X. Xu, J.J. Zheng, D.G. Truhlar, Full-dimensional potentials and state couplings and multidimensional tunneling calculations for the photodissociation of phenol, Chem. Sci. 5 (2014) 4661–14580.
- [75] C. Xie, B.K. Kendrick, D.R. Yarkony, H. Guo, Constructive and destructive

- Interference in nonadiabatic tunneling via conical intersections, J. Chem. Theo. Comput. 13 (2017) 1902–1910.
- [76] C. Xie, H. Guo, Photodissociation of phenol via nonadiabatic tunneling: Comparison of two ab initio based potential energy surfaces, Chem. Phys. Lett. 683 (2017) 222–227.
- [77] M.N.R. Ashfold, G.A. King, D. Murdock, M.G.D. Nix, T.A.A. Oliver, A.G. Sage, $\pi\sigma^*$ excited states in molecular photochemistry, Phys. Chem. Chem. Phys. 12 (2010) 1218–1238.
- [78] H. Köppel, W. Domcke, L.S. Cederbaum, Multimode molecular dynamics beyond the Born-Oppenheimer approximation, Adv. Chem. Phys. 57 (1984) 59–246.
- [79] J.W. Zwanziger, E.R. Grant, Topological phase in molecular bound states: Application to the E⊗e system, J. Chem. Phys. 87 (1987) 2954–2964.
- [80] M.S. Schuurman, D.R. Yarkony, On the locus of points of conical intersection: Seams near seams, J. Chem. Phys. 126 (2007) 044104.